Fundamental magnetotransport anisotropy in R_2Fe_{17} single crystals

Jolanta Stankiewicz*
Instituto de Ciencia de Materiales de Aragón and Departamento de Física de la Materia Condensada Consejo Superior de Investigaciones Científicas–Universidad de Zaragoza, E-50009 Zaragoza, Spain

Dmitriy Karpenkov and Konstantin P. Skokov
Faculty of Physics, Tver State University, 170002 Tver, Russia

(Received 10 August 2010; revised manuscript received 29 September 2010; published 20 January 2011)

We have measured the resistivity and Hall effect of R_2Fe_{17} (R = Y, Tb, and Gd) single crystals in the temperature T range $4 < T < 300$ K and applied magnetic fields of up to 9 T. The anomalous Hall effect (AHE) is very anisotropic in these ferromagnets. The AHE resistivity, measured with an applied magnetic field **H** perpendicular to the c axis, is very large and varies quite linearly with the longitudinal resistivity ρ, but the AHE resistivity for **H** along the hard magnetization direction (**H** $\parallel$ c axis) is much smaller and increases as ρ^2. We argue that the latter is of the intrinsic origin and is brought about by quasidegenerate Fe d levels near the Fermi level.

DOI: 10.1103/PhysRevB.83.014419 PACS number(s): 72.15.Gd, 75.30.Gw, 75.47.Np, 75.50.Bb

I. INTRODUCTION

The electronic transport properties of ferromagnetic materials have recently been the subject of many experimental and theoretical studies. In particular, the Hall effect in ferromagnets shows an anomalous term that is proportional to the magnetization of the material. It is generally accepted that skew[1] and side-jump scattering[2] contribute extrinsically to the anomalous Hall effect (AHE). They are both asymmetric and arise from spin-orbit interactions of current carriers. The intrinsic AHE,[3] independent of scattering mechanisms, is usually interpreted in terms of Berry-phase effects on conduction electrons.[4–6] Experimental studies of the AHE in dilute magnetic semiconductors, transition metals, transition-metal oxides, and spinels consistently show the importance of the intrinsic mechanism in moderately conductive materials.[7] It has been proposed that band crossings, close to the Fermi level, can resonantly enhance the Berry-phase curvature and, consequently, the anomalous Hall conductivity (AHC).[8,9] A large intrinsic AHC may follow as well from interband hopping between nearly degenerate d orbitals in ferromagnetic transition metals.[10] Thus, the physical processes behind the intrinsic AHE have not yet been clearly established. We aim to shed some light on this by studying the R_2Fe_{17} intermetallic compounds, following our earlier experiments on $Y_2Fe_{17-x}Co_x$ single crystals, which revealed the importance of the intrinsic mechanism in these alloys.[11]

The role of the extrinsic mechanism in the AHE is not well understood either. Detailed knowledge of the impurity potential is needed for a quantitative estimation of the skew-scattering contribution. Calculations of side-jump scattering are hampered by the lack of a general formalism for multiband systems. In addition, the experimental separation of various contributions to the AHE is not straightforward. The skew-scattering term of the AHE resistivity ρ_{xy} is proportional to the longitudinal resistivity ρ. However, both extrinsic side-jump scattering (which is independent of the strength and form of the impurity potential) and intrinsic band mechanisms lead to the same relation: $\rho_{xy} \propto \rho^2$. A new scaling of the AHE resistivity that also includes the residual resistivity has been proposed to identify the intrinsic and extrinsic mechanisms.[12] Frequently, first-principles calculations of the AHC are performed, and their results are compared with experimental values in order to single out the intrinsic contribution. Nevertheless, additional experimental signatures of the intrinsic AHE that have a predictable variation as a function of some well-controlled parameter are important for a clear picture. A recent demonstration that the intrinsic AHE of hcp Co single crystals depends strongly on the magnetization direction relative to the crystal axes seems significant.[13] It enables one to use the AHE anisotropy as an additional test for identifying various mechanisms behind the AHE resistivity in transition-metal ferromagnets. We make use of it in our investigation of the magnetotransport properties of R_2Fe_{17} single crystals.

The aim of this study is to find specific features of the AHE in R_2Fe_{17} single crystals in order to elucidate the role of the various mechanisms responsible for it. We choose to study these alloys because their magnetic and band-structure properties are relatively well known. The R_2Fe_{17} intermetallic compounds crystallize in a Th_2Ni_{17}-type hexagonal structure.[14] These compounds form a natural multilayer system in which the Fe layers (perpendicular to the c axis) are intercalated with dumbbell Fe pairs along the c axis. Fe atoms occupy four nonequivalent sites in the unit cell. Only the dumbbell atoms at $4f$ sites have a sufficiently high symmetry to contribute to the orbital magnetic moment. In addition, the distance between Fe atoms in the dumbbell structure is $\approx$2.39 Å, much smaller than the Fe-Fe distance (2.50 Å) in bcc Fe. A negative exchange interaction can therefore be expected between such pairs. However, positive exchange interactions with other Fe atoms force a parallel orientation of the moments of dumbbell atoms, and consequently, the Fe sublattice orders ferromagnetically, on a plane perpendicular to the c axis, in most of the R_2Fe_{17} alloys (R = rare earth, Y). The wave functions of the iron atoms at $4f$ sites quite likely overlap, giving rise to a deformation of the $3d$ band (larger magnetic polarization) and to lower electron charge density, as observed in the Mössbauer effect experiments.[15] This is in agreement with the band-structure calculations, which give the highest orbital moment for Fe atoms at the dumbbell sites.[16] The Curie

temperature lies in the range 340–510 K for $R = $ Y, Tb, and Gd.[17] The Tb and Gd rare-earth sublattices, which experience a strong exchange field, couple antiferromagnetically to the Fe sublattice in the R_2Fe_{17} alloys. A first-order magnetization process is observed at a magnetic field of about 2.5 T applied along the sixfold axis in Tb_2Fe_{17}.[18] The critical field for this transition is nearly independent of temperature up to ≈250 K even though the anisotropy constants vary with temperature, as expected from existing models.[19]

In this paper we report results of the Hall effect, resistivity, and magnetization measurements in R_2Fe_{17} ($R = $ Y, Tb, and Gd) single crystals for wide temperature and applied magnetic field ranges and for various magnetic field orientations with respect to the easy-magnetization axis. For the sake of completeness, we also include results we have previously obtained for Y_2Fe_{17} single crystals. We find a large AHE anisotropy in these systems. The AHE resistivity, measured with an applied magnetic field H in the easy plane ($\mathbf{H} \perp c$ axis), is much larger than the one for $\mathbf{H} \parallel c$ axis. More significantly, for all $T \lesssim 200$ K, the former is linear in ρ, while the latter varies as ρ^2. We finally argue that this qualitative variation of the AHE with magnetic field direction most likely comes from the intrinsic mechanism, which depends only on band-structure details and is basically anisotropic. However, an essential anisotropy is also found for the extrinsic skew-scattering contribution to AHE. We relate it to the distortion of the $3d$ bands at the dumbbell sites.

II. EXPERIMENT

All R_2Fe_{17} single crystals were grown by inductive melting of a mixture of pure components in alundum crucibles under Ar atmosphere. The mixture was rapidly heated up to the melting point and subsequently cooled down at a rate of 60–80 K/min. Further heating to approximately 1200 °C, with an annealing time of approximately 20 h was performed in order to obtain large crystalline grains. We carefully oriented the samples using x-ray back Laue diffraction. Optical metallography and atomic force microscopy were used to select specimens without grain boundaries or inclusions of extraneous phases. The magnetotransport measurements were performed on Hall bar-shaped samples with a typical size of $0.5 \times 1 \times 5\text{mm}^3$. We used a six-probe method to check for samples' homogeneity in both resistivity and Hall coefficient.[20] The relative error obtained for the resistivity is about 0.1%; absolute values are determined to within 5%. The specimens were mounted between two fixed copper plates on a sample holder to minimize thermal gradients and to avoid the effects of the large anisotropy torques on the samples when the external magnetic field was applied along the hard directions. The Hall resistivity ρ_{xy} and magnetization M were measured in a magnetic field of up to 9 T, in a temperature range from 4 to 300 K. Magnetization measurements were carried out in a superconducting quantum interference device magnetometer on the same samples that were used in the magnetotransport studies. In this way, we expected to avoid sample-shape- and domain-dependent effects when comparing results of different experiments. In addition, we relate the values of ρ_{xy} and M obtained for fields at which the magnetization is saturated. Therefore, we do not expect appreciable domain effects.

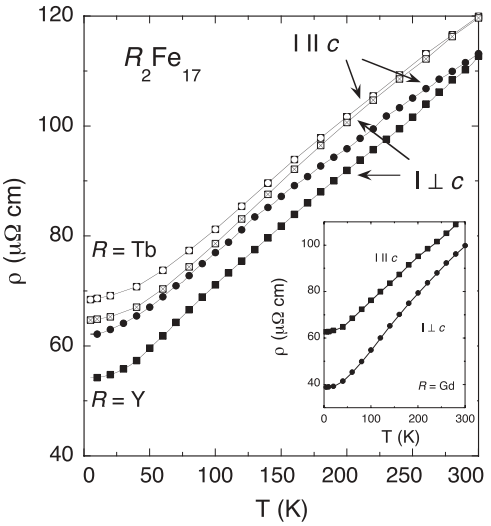

FIG. 1. Temperature dependence of the electrical resistivity in R_2Fe_{17} ($R = $ Y, Tb) single crystals for two orientations of the electrical current $\mathbf{I}$ with respect to the c axis. The solid lines are guides for the eye. The inset shows the electrical resistivity for Gd_2Fe_{17} single crystals.

III. RESULTS AND DISCUSSION

We first discuss the results from electrical resistivity measurements. Figure 1 shows how the electrical resistivity $\rho(T)$ depends on temperature T in R_2Fe_{17} single crystals. The behavior of $\rho(T)$ is typical of a ferromagnet in which phonon and spin-disorder scattering are important. The resistivity in the easy plane is lower than the resistivity along the c axis. This asymmetry is large for Gd_2Fe_{17}, where it amounts to 60%; it is approximately 15% and 6% for $R = $ Y and Tb, respectively. Since an external magnetic field suppresses spin fluctuations, the electrical resistivity decreases in magnetic field. At low temperatures, a negative magnetoresistance is approximately 3% at the highest fields applied; its magnitude decreases with increasing temperature.

We next turn to the magnetization and Hall effect results. Figures 2 and 3 show how the magnetization and Hall effect change with magnetic field at two different temperatures and for various orientations of the magnetic field with respect to the crystallographic axes of Tb_2Fe_{17} and Gd_2Fe_{17} single crystals, respectively. The Hall resistivity, which is holelike, follows the magnetization M of the samples quite closely. The experimental values of ρ_{xy} are obtained by extrapolating the Hall resistivity data, such as plotted in Fig. 2, from high magnetic fields, where the magnetization is saturated, back to $H = 0$. We note that small magnetic fields are sufficient to align magnetic moments, at least for a field on the easy plane, so this procedure is quite straightforward. The measured ρ_{xy} arises entirely from the AHE since the ordinary contribution to the Hall effect is negligible in our samples. All data points for ρ_{xy} in Figs. 4–6 are obtained when the magnetization is saturated. For $GdFe_{17}$, where the magnetization is not completely saturated at 5 K along the hard direction even for a field of 9 T, we use the law of approach to saturation[21] to estimate M_s. In Fig. 4, we plot the Hall resistivity of R_2Fe_{17} ($R = $ Y, Tb, and Gd) versus the total longitudinal

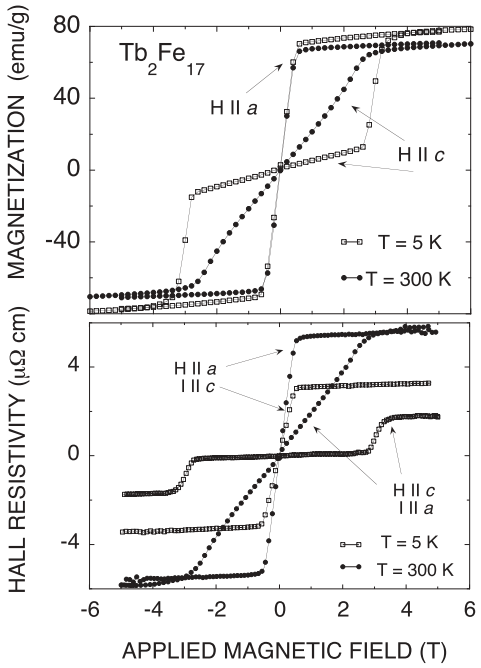

FIG. 2. Magnetization and Hall resistivity as a function of magnetic field for Tb_2Fe_{17} single crystals at 5 and 300 K. The solid line is a guide for the eye.

resistivity ρ ($\rho = \rho_{xx}$), using data obtained for $\rho_{xy}(T)$ and $\rho(T)$ in the temperature range from 4 to 300 K. The range of the longitudinal resistivity is quite limited for some samples. As the present state of the art for single-crystal growth of intermetallic ferromagnets stands, it is difficult to obtain materials with a small residual resistivity and, consequently, to have a larger span for the variation of the resistivity with

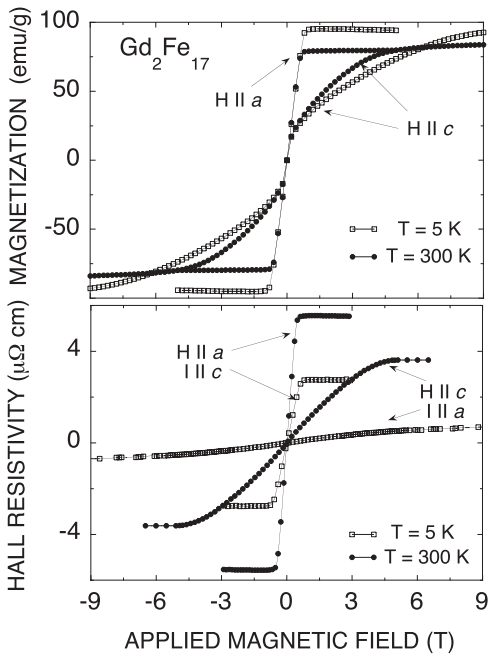

FIG. 3. Magnetization and Hall resistivity as a function of magnetic field for Gd_2Fe_{17} single crystals at 5 and 300 K. The solid line is a guide to the eye.

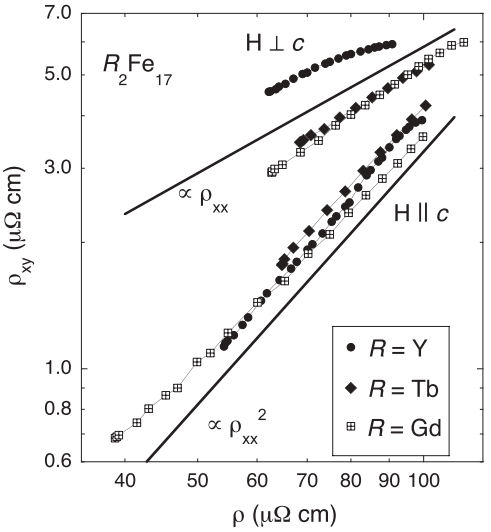

FIG. 4. Hall resistivity of R_2Fe_{17} single crystals as a function of the longitudinal resistivity for different orientations of the applied magnetic field with respect to the crystallographical axes. The solid lines show a linear and a quadratic in ρ variation.

temperature. In spite of this, clear straight lines in this log-log plot are found. The variation of ρ_{xy} with ρ depends crucially on orientation: The Hall resistivity drops by a factor of $\sim$4 as the magnetization is tilted from the easy ab plane to the c axis at low temperatures. In addition, the AHE resistivity varies almost linearly with ρ for **M** in the ab plane but follows a ρ^2 dependence for **M** in the hard direction. This is so for each of the three alloys we have studied.

We analyze the anomalous Hall resistivity data following a procedure outlined in Refs. 22 and 23 and also used by us to treat Y_2Fe_{17} data.[11] Consider the relation between the AHE and the longitudinal resistivity of the form $\rho_{xy} = a'(M_s)\rho + b'(M_s)\rho^2$. Coefficients $a'(M_s)$ and $b'(M_s)$ are some function of the spontaneous magnetization. The first term stands for the skew-scattering contribution, which is usually linear in the magnetization.[22] With a simple approximation, $a'(M_s) = aM_s(T)/M_s^o$, and plotting $(\rho_{xy}/\rho)[M_s^o/M_s(T)]$ versus ρ, we can obtain the coefficient a, which is assumed to be independent of temperature. Here $M_s^o = M_s(T = 0)$. The second term represents the intrinsic contribution; in particular, the AHC, $\sigma_{xy}^a = \rho_{xy}/\rho^2$, is given by $b'(M_s)$. Since $\sigma_{xy}^a \propto M_s$, as has also been found for ferromagnetic Mn_5Ge_3,[22] the slope of $(\rho_{xy}/\rho)[M_s^o/M_s(T)]$ versus ρ yields the low-temperature value of the AHC. The $\rho_{xy} \propto \rho^2$ relation is also predicted for extrinsic side-jump scattering. As discussed below, this mechanism is, however, unimportant in our samples.

We have also tried an alternative scaling of the AHE in R_2Fe_{17} single crystals, namely, $\rho_{xy} = (a'\rho_0 + a''\rho_0^2) + b'\rho^2$, that has been recently proposed for epitaxial Fe films.[12] In this model, the external contributions to the AHE depend only on the residual, temperature-independent resistivity ρ_0. Consequently, the experimental AHC, $\sigma_{xy}^a \approx \rho_{xy}/\rho^2$, should vary linearly with σ^2 ($\sigma = 1/\rho$) and not with σ as we assume above. We found, however, that a $\rho_{xy} = f(\rho)$ scaling, in which the skew and side-jump terms are proportional to the total, not to the residual resistivity, is much better in our case. This is clearly seen in Fig. 5, where both scalings are displayed.

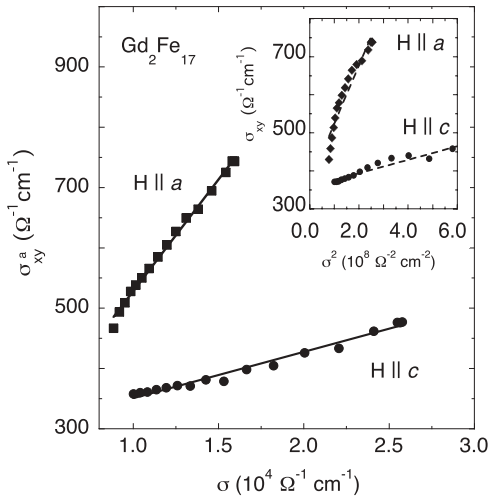

FIG. 5. Anomalous Hall conductivity (AHC) of Gd_2Fe_{17} single crystals as a function of the longitudinal conductivity for different orientations of the applied magnetic field with respect to the crystallographical axes. The solid lines show a linear fit to the data points. The inset exhibits AHC as a function of the square of the longitudinal conductivity for the same crystals.

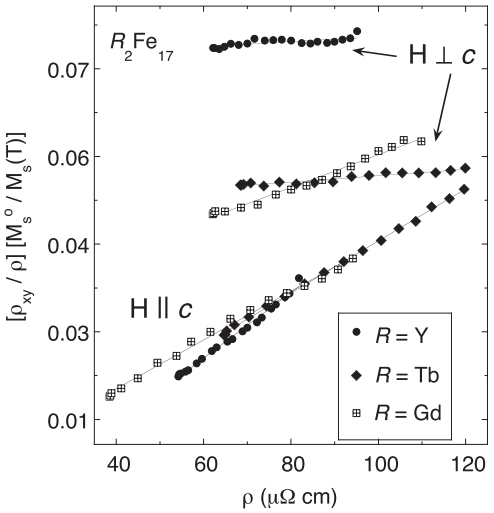

FIG. 6. Plot of $(\rho_{xy}/\rho)[M_s^o/M_s(T)]$ versus ρ for R_2Fe_{17} single crystals, with $\mathbf{H} \perp c$ axis and $\mathbf{H} \parallel c$ axis. The solid lines are linear fits to the data points.

How $(\rho_{xy}/\rho)[M_s^o/M_s(T)]$ varies with ρ in R_2Fe_{17} single crystals is shown in Fig. 6. This quantity is highly anisotropic. When $\mathbf{M}$ lies on the easy plane, $\rho_{xy}M_s^o/\rho M_s(T)$ is constant for $T \lesssim 150$ K in Y_2Fe_{17} and for $T \lesssim 250$ K in Tb_2Fe_{17}. This is not quite so for Gd_2Fe_{17}, where it shows some slight variation with ρ. However, when $\mathbf{M}$ is lined up along the hard direction, $\rho_{xy}M_s^o/\rho M_s(T)$ varies linearly with ρ for all the alloys studied. Skew scattering is therefore important for the easy-plane AHE in R_2Fe_{17}, but the intrinsic mechanism seems to determine the AHE along the hard axis. These conclusions agree with the results of first-principles calculations for hcp Co, which show strong anisotropy of the intrinsic AHE.[13] In addition, the orientation dependence of the AHE in R_2Fe_{17} enables one to discriminate between intrinsic and side-jump contributions. The latter leads to an isotropic Hall current,[2] but no contribution of the form $\rho_{xy} \propto \rho^2$ is seen when M lies on the easy plane, at least for $R =$ Y and Tb. We therefore infer that side-jump scattering is negligible in the alloys we are reporting on. This agrees with a prediction that such a contribution to the AHE is much smaller than the intrinsic one in ferromagnetic metals.[24]

Table I gives AHE parameters with their corresponding errors obtained from the linear fittings to the data shown in Fig. 6. The magnitude of the skew term as well as its orientation dependence are surprising. We find that the skew-scattering coefficient a (see Table I) for R_2Fe_{17} is more than one order of magnitude larger than the ones found for metallic[23] or half-metallic ferromagnets.[25] Furthermore, it is large for magnetic fields in the easy plane and is much smaller for a perpendicular orientation. Although a quantitative estimation of the skew-scattering contribution is a difficult task, it is expected to be isotropic.[1] We found much the same behavior of the AHE in $Y_2Fe_{17-x}Co_x$ single crystals with $x \lesssim 2$.[11] The observed anisotropy may come from a likely deformation of the d bands at dumbbell sites. This favors skew scattering of charge carriers for M in the easy plane. Interestingly, no such effect is found in $R_2Fe_{14}B$ single crystals,[26] where the shortest Fe-Fe interatomic distance is nearly the same as in R_2Fe_{17}.[27] However, such pairs for $R_2Fe_{14}B$ are found in a plane perpendicular to the c axis, instead of along the c axis as in R_2Fe_{17}.

We now turn to data obtained for $\mathbf{H}$ along the hard direction. As argued, the intrinsic contribution, related to Berry-phase effects on conduction electrons, dominates the AHE in this configuration. The skew-scattering parameter a is at least one order of magnitude smaller than the one found for for M on the easy plane. For σ_{xy}^a, we obtain values between 505 and 390 $(\Omega\ \text{cm})^{-1}$ as we move from $R =$ Y to $R =$ Gd. These values are close to theoretical predictions for the intrinsic Hall conductivity, which give for R_2Fe_{17} $\sigma_{xy}^a \approx e^2/(ha_0) \approx$ 480 $(\Omega\ \text{cm})^{-1}$, where a_0 is the lattice constant.[10,28] We note that the AHC anisotropy is quite a bit smaller for Gd_2Fe_{17} than

TABLE I. Anomalous Hall resistivity parameters obtained for R_2Fe_{17} single crystals used in this study. a is the skew scattering coefficient, and σ_{xy}^a is the low-temperature value of the intrinsic Hall conductivity.

	$\mathbf{M}_s \perp c$		$\mathbf{M}_s \parallel c$	
	a	σ_{xy}^a $(\Omega\ \text{cm})^{-1}$	a	σ_{xy}^a $(\Omega\ \text{cm})^{-1}$
Y_2Fe_{17}	$0.072 \pm 5\%$	$30 \pm 70\%$	$-0.006 \pm 30\%$	$505 \pm 10\%$
Tb_2Fe_{17}	$0.047 \pm 5\%$	$50 \pm 10\%$	$0.0009 \pm 25\%$	$420 \pm 5\%$
Gd_2Fe_{17}	$0.030 \pm 10\%$	$250 \pm 15\%$	$0.003 \pm 30\%$	$390 \pm 10\%$

for Y_2Fe_{17} or Tb_2Fe_{17}. However, it is clear that the overall behavior of the Hall effect is dominated by the Fe sublattice in the R_2Fe_{17} alloys.

The main contribution to the intrinsic AHE comes from electronic states corresponding to a few high-symmetry points in the Brillouin zone for which the orbital moment is not quenched. Only Fe ions at 4*f* sites have an orbital magnetic moment. The electronic states in the vicinity of the Fermi energy in R_2Fe_{17} alloys are mostly of 3*d* orbital character. A hexagonal crystal field partially removes their degeneracy, leaving the d_{zx} and d_{yz} orbitals still degenerate. As shown by band-structure calculations carried out within the tight-binding model,[29] the d_{xz} and d_{yz} orbitals are split by a combined effect of spin-orbit and exchange interactions. This splitting is very small when $\mathbf{M}_s$ is along the *c* axis because of a nonzero orbital moment and strong effective field experienced by the Fe ions at the dumbbell. In addition, the d_{zx}–d_{yz} subband happens to lie close to the Fermi level. Although we do not know its energy dispersion, it is quite plausible that variations of the total Berry curvature, coming from avoided crossings of theses states near the Fermi energy, resonantly enhance the AHC amplitude when $\mathbf{M}_s$ is along the *c* axis. This scenario would also explain the orientation dependence of the intrinsic AHC. As shown in Ref. 13, such dependence is related to quasidegenerate states close to the Fermi energy that avoid crossing upon magnetization rotation and, consequently, give rise to sharp variations in Berry curvature.

A different mechanism for the intrinsic AHE, in which hopping between the d_{zx} and d_{yz} orbitals gives rise to an anomalous velocity and thus to the AHE, has been proposed.[10] However, the observed anisotropy of the intrinsic AHC does not arise in this model as naturally as in the one we discuss above.

In summary, we find that both extrinsic and intrinsic contributions to the AHE in the ferromagnetic R_2Fe_{17} are highly anisotropic. Nearly degenerate *d* levels of Fe ions, which lie close to the Fermi energy, are most likely at the root of the variation of the intrinsic anomalous Hall conductivity with orientation. On the other hand, a distortion of the *d* bands may account for the observed anisotropy of skew scattering. Calculations of these effects would help justify the inferences we make.

ACKNOWLEDGMENTS

We acknowledge support from Grant No. MAT2008/03074 from the Ministerio de Ciencia e Innovación of Spain. Additional support from Diputación General de Aragón (DGA-IMANA) and from Caja Inmaculada–DGA Grant No. CB1–09 (Programa Europa XXI) is also acknowledged.

*jolanta@unizar.es

[1] J. Smit, Physica (Amsterdam) **21**, 877 (1955).
[2] L. Berger, Phys. Rev. B **2**, 4559 (1970).
[3] R. Karplus and J. M. Luttinger, Phys. Rev. **95**, 1154 (1954).
[4] T. Jungwirth, Q. Niu, and A. H. MacDonald, Phys. Rev. Lett. **88**, 207208 (2002).
[5] Y. Yao, L. Kleinman, A. H. MacDonald, J. Sinova, T. Jungwirth, D.-S. Wang, E. Wang, and Q. Niu, Phys. Rev. Lett. **92**, 037204 (2004).
[6] R. Mathieu, A. Asamitsu, H. Yamada, K. S. Takahashi, M. Kawasaki, Z. Fang, N. Nagaosa, and Y. Tokura, Phys. Rev. Lett. **93**, 016602 (2004).
[7] N. Nagaosa, J. Sinova, S. Onoda, A. H. MacDonald, and N. P. Ong, Rev. Mod. Phys. **82**, 1539 (2010).
[8] Z. Fang, N. Nagaosa, K. S. Takahashi, A. Asamitsu, R. Mathieu, T. Ogasawara, H. Yamada, M. Kawasaki, Y. Tokura, and K. Terakura, Science **302**, 92 (2003).
[9] S. Onoda, N. Sugimoto, and N. Nagaosa, Phys. Rev. Lett. **97**, 126602 (2006).
[10] H. Kontani, T. Tanaka, and K. Yamada, Phys. Rev. B **75**, 184416 (2007).
[11] J. Stankiewicz and K. P. Skokov, Phys. Rev. B **78**, 214435 (2008); J. Stankiewicz, K. P. Skokov, G. Khokholkov, J. Bartolomé, and Y. G. Pastushenkov, IEEE Trans. Magn. **44**, 4506 (2008).
[12] Y. Tian, L. Ye, and X. Jin, Phys. Rev. Lett. **103**, 087206 (2009).
[13] E. Roman, Y. Mokrousov, and I. Souza, Phys. Rev. Lett. **103**, 097203 (2009).
[14] D. Givord, R. Lemaire, J. M. Moreau, and E. Roudaut, J. Less Common Met. **29**, 361 (1972).
[15] P. C. M. Gubbens, J. J. van Loef, and K. H. J. Buschow, J. Phys. Colloq. **35**, C6-617 (1974).
[16] R. Coehoorn, Phys. Rev. B **39**, 13072 (1989); R. F. Sabiryanov and S. S. Jaswal, *ibid.* **57**, 7767 (1998).
[17] K. Takeda, T. Maeda, and T. Katayama, J. Alloys Compd. **281**, 50 (1998).
[18] R. Verhoef, P. H. Quang, R. J. Radwański, C. Marquina, and J. J. M. Franse, J. Magn. Magn. Mater. **104-107**, 1473 (1992).
[19] M. D. Kuz'min, Y. Skourski, K. P. Skokov, K.-H. Müller, and O. Gutfleisch, Phys. Rev. B **77**, 132411 (2008).
[20] ASTM, Standard Test Methods for Measuring Resistivity and Hall Coefficient and Determining Hall Mobility a Single-Crystal Semiconductors, ASTM F76-86, 31 October 1986.
[21] S. Chikazumi, *Physics of Magnetism* (Wiley, New York, 1964), pp. 274–280.
[22] C. Zeng, Y. Yao, Q. Niu, and H. H. Weitering, Phys. Rev. Lett. **96**, 037204 (2006).
[23] B. C. Sales, R. Jin, and D. Mandrus, Phys. Rev. B **77**, 024409 (2008).
[24] P. Nozieres and C. Lewiner, J. Phys. (France) **34**, 901 (1973).
[25] M. J. Otto, R. A. M. van Woerden, P. J. van der Valk, J. Wijngaard, C. F. van Bruggen, and C. Haas, J. Phys. Condens. Matter **1**, 2351 (1989).
[26] J. Stankiewicz, J. Bartolomé, and S. Hirosawa, Phys. Rev. B **64**, 094428 (2001).
[27] J. F. Herbst, Rev. Mod. Phys. **63**, 819 (1991).
[28] T. Miyasato, N. Abe, T. Fujii, A. Asamitsu, S. Onoda, Y. Onose, N. Nagaosa, and Y. Tokura, Phys. Rev. Lett. **99**, 086602 (2007).
[29] K. Kulakowski and A. del Moral, Phys. Rev. B **50**, 234 (1994).